

**INVESTIGATION FOR LATERITE DEPOSITS USING 2D ELECTRICAL
RESISTIVITY IMAGING METHOD IN OVIA NORTH EAST AREA OF EDO
STATE.**

BY

NWANKWOR IKECHUKWU

PSC1707826

**A PROJECT WRITTEN IN THE DEPARTMENT OF PHYSICS AND SUBMITTED
TO THE DEPARTMENT OF PHYSICS IN PARTIAL FULFILMENT OF THE
REQUIREMENT FOR THE AWARD OF BACHELOR OF SCIENCE DEGREE IN
PHYSICS, UNIVERSITY OF BENIN, BENIN CITY, NIGERIA.**

JANUARY, 2023.

CERTIFICATION

I hereby certify that this project was carried out under my supervision by **NWANKWOR IKECHUKWU**, a final year student of Department of Physics, Faculty of Physical Sciences, University of Benin, Benin City, Edo State, Nigeria.

Dr. JOHN AIREN
Supervisor

Date

PROF. O. D. OSAHON
Head of Physics Department

Date

.....
EXTERNAL EXAMINER

.....
Date

DEDICATION

This project work is dedicated to God Almighty who made everything possible, who gave me the strength to carry on till the end.

ACKNOWLEDGEMENTS

My warmest appreciation goes to God almighty who have been wonderful and faithful to me throughout my stay in the University of Benin.

My profound gratitude also goes to my project supervisor Airen John (Ph.D.) for his scrutiny, guidance and encouragement throughout the stages of my project work.

Immense gratitude also goes to my Mom Mrs. Patience Nwankwor for her financial support, encouragement and prayers.

I also want to thank my beloved brother, the person of Mr. Nwankwor Arinze for love and support. May God grant you all your heart desire.

ABSTRACT

A 2-D resistivity survey was carried out in UBTH, Edo State, a sedimentary terrain of South-South Nigeria. The Wenner-Schlumberger alpha electrode configuration was engaged throughout in this study. To obtain a good 2-D picture of the subsurface, the coverage of the measurements must be 2-D as well. The equipment used to take the resistivity values was the Pasi Earth Resistivity meter. The data from each 2-D survey line was inverted independently with RES2DINV to give 2-D cross-sections with RMS error of 8.15%.

A contoured pseudosection conveys a qualitative two-dimensional resistivity variation with depth within the subsurface. The inverted model resistivity sections created models for the subsurface resistivity using an iterative smoothness constrained least square inversion and are interpreted to generate the subsurface geologic characteristics.

Results from 2-D inverted resistivity section showed that the first line with resistivity of laterites ranges from 800-1500 Ω m, while that of lateritic soils ranges from 120-750 Ω m from depth 2-10m. It can be seen that the resistivity of the sub-surface soils corresponds with the resistivity of laterites, thereby confirming the existence of laterites deposits in the survey area. From the resistivity block section obtained from line 2, it can be seen that the survey area has laterite deposits and lateritic soils, the top of the soil is composed of laterites and as we go deeper, it becomes lateritic soil because of the increase in the composition of non-lateritic materials with depth.

TITLE PAGE

Certification	I	
Dedication		II
Acknowledgement	III	
Abstract		IV

CHAPTER ONE

1.0 Introduction	1	
1.1 Geophysical Exploration	1	
1.2 Laterite Soil	1	
1.3 Properties of Laterites		3
1.4 Characteristics of Laterite Soil	4	
1.5 Aim and Objectives	4	
1.6 Location of Study Area		5
1.7 Geology of Study Area		6

CHAPTER TWO

2.0 Literature Review	8	
2.1 Electrical Properties of Rocks		8
2.2 Electrical Resistivity Survey		12
2.2.1 Currents and voltages in a uniform Earth	16	
2.2.2 Two electrode current sources	18	
2.2.3 Apparent resistivity	21	
2.2.4 The essence of interpreting resistivity surveys is to find the true distribution of intrinsic resistivities by interpreting the pattern of apparent resistivities that were measured.	22	
2.2.5 Anisotropic ground	23	
2.3 Electrode Configuration in Resistivity Survey	25	

CHAPTER THREE

3.0 Materials and Methodology	29	
3.1 Materials		29
3.2 Equipment Used For the Field Work	29	
3.3 Field Survey Method	32	
3.4 Measurement Procedure	33	
3.4.1 Field calculations		34

CHAPTER FOUR

4.0	Result and Discussion	35
4.1	Result	35
4.2	Interpretation of Results	40

CHAPTER FIVE

5.0	Findings, Conclusion and Suggestion For Further Studies	45
5.1	Findings	45
5.3	Suggestion for Further Studies	46

REFERENCES

LIST OF FIGURES

Figure 1.1:	Showing laterite	4
Figure 1.2:	Map of the study area	6
Figure 2.1	Electric potential inside the earth	18
Figure 2.2:	current electrode	18
Figure 2.3:	graph of the current flow into the ground flows through rock at depths shallower than or equal to the current electrode spacing.	19
Figure 2.4:	voltage Electrode	20
Figure 2.5:	Array configuration and their geometric factors	23
Figure 2.6:	coefficient of anisotropy for layered rocks (after Keller and Frischknecht, 1992)	24
Figure 2.7:	Electrode configuration in electrical resistivity surveys	25
Figure 2.8:	Wenner Array	27
Figure 2.9:	Schlumberger Array	28
Figure 3.1:	Pasi Earth Resistivity Meters	31
Figure 3.2:	A Global Positioning System	31
Figure 3.3:	Measuring Tape and electrodes.	32
Figure 3.4:	Hammer	32
Figure 3.5:	Principle of resistivity measurement	34
Figure 4.1:	Traverse 1 showing the inverse resistivity section	42
Figure 4.2:	Traverse 2 showing the inverse resistivity section	43
Figure 4.3:	Traverse 3 showing the inverse resistivity section	44

LIST OF TABLES

Table 2.1:	Typical electrical resistivities of earth	12
Table 2.2:	the proportion for the six paths (current path 1 is the top-most path and 6 is the bottom-most path).	20
Table 4.1:	2-D Wenner-Schlumberger Electrical Resistivity	

Field Record – Traverse one	35
Table 4.2: 2-D Wenner-Schlumberger Electrical Resistivity	
Field Record – Traverse Two	37
Table 4.3: 2-D Wenner-Schlumberger Electrical Resistivity	
Field Record – Traverse three	39
Table 4.4: Resistivity values of common rocks, soil materials and chemical	41

CHAPTER ONE

INTRODUCTION

1.1 GEOPHYSICAL EXPLORATION

Exploration geophysics plays a major role in the areas of mineral and petroleum exploration, marine geology, groundwater exploration, and engineering construction, wherein its primary aim is to add an extra dimension to geological information. In its basic essentials it is a method of *geological exploration*, using instruments whose function is to record changes in the physical properties of rocks in the subsurface. It therefore involves the application of principles of several physical sciences and relates to the measurement of rock properties such as density, velocity, susceptibility, and resistivity and involves the drawing of deductions about the rock types and their geological configurations. There is also some prediction involved in terms of inferring the probability of the presence of mineral deposits, hydrocarbons, and groundwater. The purpose of this study is to search for laterite which is of immense economic value.

1.2 LATERITE SOIL

Laterites are soil types rich in iron and aluminum, formed in hot and wet tropical areas (Tardy, 1992). Nearly all laterites are rusty-red because of iron oxides. They develop by intensive and long-lasting weathering of the underlying parent rock. Tropical weathering is a prolonged process of chemical weathering which produces a wide variety in the thickness, grade, chemistry and ore mineralogy of the resulting soils (Tardy, 1992). The majority of the land areas with laterites ore are between the tropics of Cancer and Capricorn (Tardy, 1992). Historically, laterite was cut into brick-like shapes and used in monument building (Sivaramakrishnan et al., 2015). Since the mid-1970s trial sections of bituminous surfaced, low-volume roads have used laterite in place of stone as a base course. Thick laterite layers are porous and slightly permeable, so the layers can function as aquifers in rural areas. Locally available laterites are used in an acid solution, followed by precipitation to remove phosphorus and heavy metals at sewage treatment facilities (Sivaramakrishnan et al., 2015).

Laterites are a source of aluminum ore; the ore exists largely in clay minerals and the hydroxides, gibbsite, boehmite, and diaspore, which resembles the composition of bauxite (Pidlisecky et al., 2006). In Northern Ireland they once provided a major source of iron and aluminum ores (Pidlisecky et al., 2006). Laterite ores also were the early major source of nickel. Francis Buchanan-Hamilton first described and named a laterite formation in southern India in 1807 (Sivaramakrishnan et al., 2015). He named it laterite from the Latin word *later*, which means a brick; this rock can easily be cut into brick-shaped blocks for building. Laterites can be either soft or easily broken into smaller pieces, or firm and physically resistant.

Laterites are formed from the leaching of parent sedimentary (sandstones, clays, lime stones); metamorphic rocks (schists, gneisses, migmatites); igneous rocks (granites, basalts, gabbros, peridotites); and mineralized proto-ores; which leaves the more insoluble ions, predominantly iron and aluminum. An essential feature for the formation of laterite is the repetition of wet and dry seasons. The mineralogical and chemical compositions of laterites are dependent on their parent rocks. Laterites vary significantly according to their location, climate and depth. Laterites are widely used to build blocks, build roads, as aquifers in water supply, water treatment etc. (Adekunle and Adeniyi, 2015)

1.3 PROPERTIES OF LATERITES

Laterite is both a soil and a rock type, rich in iron and aluminum and is commonly considered to have formed in hot and wet tropical areas. Nearly all laterites are of rusty-red coloration, because of high iron oxide content. They develop by intensive and prolonged weathering of the underlying parent rock. Laterites are formed from the leaching of parent sedimentary rocks, metamorphic rocks, and igneous rocks and mineralized photo-ores which leaves the more insoluble ions, predominantly iron and aluminium. The mechanism of leaching involves acid dissolving the host mineral laterites followed by hydrolysis and precipitation of insoluble oxides and suitates of iron, aluminium and silica under high temperature conditions of a humid subtropical monsoon climate. An essential feature of the formation of laterites is the

repetition of wet and dry seasons. Rocks are leached by percolating rain water during the wet season; the resulting solution containing the leached ions is brought to the surface by capillary action during the dry season. These ions form soluble salt compounds which dry on the surface; these salts are washed away during the next wet season the significant features of the lateritic soils are their unique color, poor fertility, and high clay content and lower cation exchange capacity. In addition, lateritic soils possess a great amount of iron and aluminum oxides.

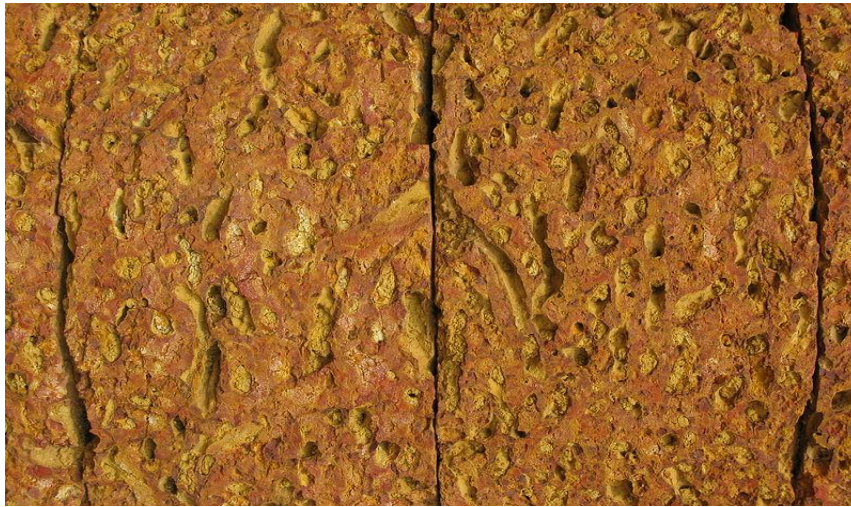


Figure 1.1: Showing laterite

In laterite areas where a high level of culture once prevailed, ruins often disclose laterite used as a building stone. Open cisterns, sewers, headwalls, culverts, flagstones, quays, moles, and breakwaters of laterite have functioned successfully for hundreds of years.

1.4 CHARACTERISTICS OF LATERITE SOIL

- i. Laterite Soils are leached Soils because alternating dry and wet spells cause the soluble silica to be removed.
- ii. These Soils are acidic in nature and coarse and crumbly in texture.
- iii. The proportion of lime and silica is reduced when leaching takes place.

1.5 AIM AND OBJECTIVES

The aim of this project is to investigate for laterites deposits using 2-D electrical resistivity imaging method in the University of Benin, Benin City Edo State.

The objectives of this work are to;

1. carry out a 2-D geoelectrical investigation for Laterites deposit in the study area
2. characterize the subsurface and also determine the depths and the conductive properties of laterites.

1.6 LOCATION OF STUDIE AREA

Ovia northeast local government area is one of the eighteen local government areas in Edo State of Nigeria. The local government area was created from the district council under the local government law in 1976, the local government which lies across the larger part of the local government. Ovia North East local government area is one of the largest local area in Edo State in term of land mass. The geological setting in the area of study consists of the coastal plain sands sometimes referred to as Benin sands of the Benin Formation in Nigeria. The Benin sands are partly marine, partly deltaic and partly lagoonal (Ogunsanwo, 1989), all indications of a shallow water environment of deposition (Short and Stauble, 1967). Benin City is underlain by sedimentary formation. The formation is made up of top reddish clayey sand capping highly porous fresh water bearing loose pebbly sands, and sandstone with local thin clays and shale interbeds which are considered to be of braided stream origin. Sands, sandstones and clays vary in colour from reddish brown to pinkish yellow on weathered surfaces to white in the deeper fresh surfaces. Limonitic coatings are responsible for the brown reddish-yellowish colour. The formation is covered with loose brownish sand (quaternary drift) varying in thickness and is about 800 m thick; almost all of which is water bearing with water level varying from about 20 m to 52 m (Kogbe, 1989). The coastal plain sands in the study area is bounded by Alluvium and Mangrove swamps before it, and afterwards by the Bende Ameki Formation and Imo clay-shale group. The Benin formation encapsulates sedimentary rocks of ages between Palaeocene to recent and contains about 90% of sandstone and shale intercalation. It is coarse grained locally fine grained in some areas,

poorly sorted, subangular to well-rounded and bears lignite streaks and wood fragment (Loke and Barker, 1996).

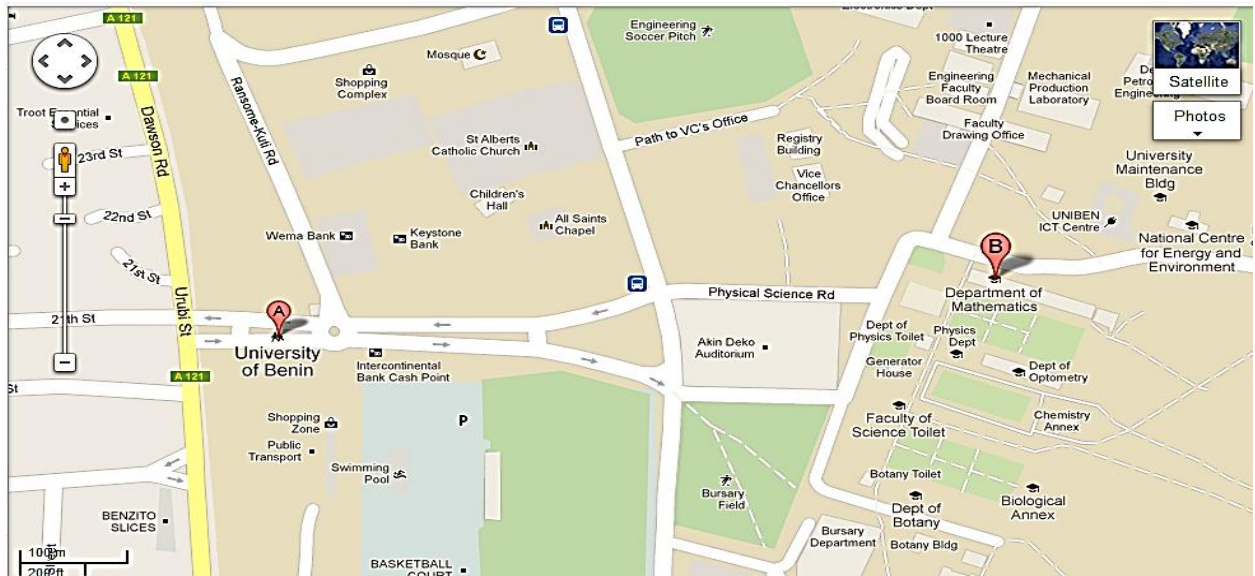


Figure 1.2: Map of the study area

1.7 GEOLOGY OF STUDY AREA

Geology of the study area is described in the geology of Niger delta. Niger delta is one of the ten major sedimentary basins of Nigeria. The others are Abakaliki basin, Anambra Basin, Benue trough, Bida basin, Bornu-Chad basin, Dahomey basin, Gongola basin, Sokoto basin and Yola basement complex. These are Western end of the Cameroun volcanic zone, Northern Nigeria massif and the eastern end of West African massif. The basins and basement complex are shown in figure 1.2 The Niger Delta complex basin is situated on the Gulf of Guinea on the west coast of Central Africa. It built out into the Atlantic Ocean at the mouth of the Niger-Benue river system during the tertiary. The maximum sediment thickness is at the central part of the delta within the greater Ughelli megastructure. The thickness is about 12 kilometers.

The formation of Niger delta basin and others started with the break of the central African-south American part of the Gondwana super continent. This took place in the Mesozoic. It is along a series of rift zones of different orientations that met in a triple junction on the present gulf of Guinea. Two of the arms, which followed the south eastern and south western coasts of Nigeria developed into collapsed continental margins of south.

CHAPTER TWO

LITERATURE REVIEW

2.1 ELECTRICAL PROPERTIES OF ROCKS

All materials, including soil and rock, have an intrinsic property, resistivity that governs the relation between the current density and the gradient of the electrical potential. Variations in the resistivity of earth materials, either vertically or laterally, produce variations in the relations between the applied current and the potential distribution as measured on the surface, or thereby reveal something about the composition, extent, and physical properties of the subsurface materials. The various electrical geophysical techniques distinguish materials through whatever contrast exists in their electrical properties. Materials that differ geologically, such as described in a lithologic log from a drill hole, may or may not differ electrically and, therefore, may or may not be distinguished by an electrical resistivity survey. Properties that affect the resistivity of a soil or rock include porosity, water content, composition (clay mineral and metal content), salinity of the pore water, and grain size distribution. In an electrically conductive body that lends itself to description as a one-dimensional body, such as an ordinary wire, the relationship between the current and potential distribution is described by Ohm's law:

$$V = IR \quad (2.1)$$

Where

V= Voltage

I= Current

R= Resistance

The resistance (R) of a length of wire is given by

$$R = \rho \frac{L}{A} \quad (2.2)$$

Where

ρ = resistivity of the medium composing the wire,

L = length,

A = area of the conducting cross section

Note that if R is expressed in ohms (Ω), the resistivity has the dimensions of ohms multiplied by a unit of length. It is commonly expressed in Ωm but may be given in $\Omega\text{-cm}$ or $\Omega\text{-ft}$. The conductivity (σ) of a material is defined as the reciprocal of its resistivity (ρ). Resistivity is thus seen to be an intrinsic property of a material, in the same sense that density and elastic moduli are intrinsic properties. In most earth materials, the conduction of electric current takes place virtually entirely in the water occupying the pore spaces or joint openings, since most soil- and rock-forming minerals are essentially nonconductive. Clays and a few other minerals, notably magnetite, specular hematite, carbon, pyrite, and other metallic sulfides, may be found in sufficient concentration to contribute measurably to the conductivity of the soil or rock. Water, in a pure state, is virtually nonconductive but forms a conductive electrolyte with the presence of chemical salts in solution, and the conductivity is proportional to the salinity. The effect of increasing temperature is to increase the conductivity of the electrolyte. When the pore water freezes, there is an increase in resistivity, perhaps by a factor of 104 or 105, depending on the salinity. However, in soil or rock, this effect is diminished by the fact that the pore water does not all freeze at the same time, and there is usually some unfrozen water present even at temperatures considerably below freezing. The presence of dissolved salts and the adsorption of water on grain surfaces act to reduce the freezing temperature. Even so, electrical resistivity surveys made on frozen ground are likely to encounter difficulties because of the high resistivity of the frozen surface layer and high

contact resistance at the electrodes. On the other hand, the effect of freezing on resistivity makes the resistivity method very useful in determining the depth of the frozen layer. It is very helpful in the interpretation of such surveys to have comparison data obtained when the ground is unfrozen. Since the conduction of current in soil and rock is through the electrolyte contained in the pores, resistivity is governed largely by the porosity, or void ratio, of the material and the geometry of the pores. Pore space may be in the form of intergranular voids, joint or fracture openings, and blind pores, such as bubbles or vugs. Only the interconnected pores effectively contribute to conductivity, and the geometry of the interconnections, or the tortuosity of current pathways, further affects it. The resistivity ρ of a saturated porous material can be expressed as

$$\rho = F\rho_w \quad (2.3)$$

Where

F = formation factor,

ρ_w = resistivity of pore water.

The formation factor is a function only of the properties of the porous medium, primarily the porosity and pore geometry. An empirical relation, Archie's Law, is sometimes used to describe this relationship:

$$F = a\phi^{-m} \quad (2.4)$$

Where

“a” and “m” = empirical constants that depend on the geometry of the pores,

ϕ = porosity of the material.

Values of ‘a’ in the range of 0.47 to 2.3 can be found in the literature. The value of m is generally considered to be a function of the kind of cementation present and is reported to vary from 1.3 for completely uncemented soils or sediments to 2.6 for highly cemented rocks,

such as dense limestones. Equations 3 and 4 are not usually useful for quantitative interpretation of data from surface electrical surveys but are offered here to help clarify the role of the pore spaces in controlling resistivity. Bodies of clay or shale generally have lower resistivity than soils or rocks composed of bulky mineral grains. Although the clay particles themselves are nonconductive when dry, the conductivity of pore water in clays is increased by the desorption of exchangeable cations from the clay particle surfaces. Table 1 shows some typical ranges of resistivity values for manmade materials and natural minerals and rocks, similar to numerous tables found in the literature (Van Blaricon 1980; Telford et al. 1976; Keller and Frischknecht 1966). The ranges of values shown are those commonly encountered but do not represent extreme values. It may be inferred from the values listed that the user would expect to find in a typical resistivity survey low resistivities for the soil layers, with underlying bedrock producing higher resistivities. Usually, this will be the case, but the particular conditions of a site may change the resistivity relationships. For example, coarse sand or gravel, if it is dry, may have a resistivity like that of igneous rocks, whereas a layer of weathered rock may be more conductive than the soil overlying it. In any attempt to interpret resistivities in terms of soil types or lithology, consideration should be given to the various factors that affect resistivity.

Table 2.1: Typical electrical resistivities of earth

Material	Resistivity
Clay	1-20
Sand, wet to moist	20-200
Shale	1-500
Porous limestone	100-1000
Dense limestone	1000-1,000,000
Metamorphic rock	50-1,000,000
Igneous rocks	100-1,000,000

2.2 ELECTRICAL RESISTIVITY SURVEY

Soil electrical resistivity is a measure of how much the soil resists the flow of electricity. Soil resistivity is a basic parameter and one of the most important methods for the design of effective grounding and lightning Prevention/protection systems. In addition, resistivity profiling can yield information on characteristics (including depth) of different layers in the subsurface. The resistivity of rocks or soils is in general a complicated function of their porosity, permeability, ionic content of pore fluids, and mineralization. In most rock materials, the porosity and the ionic content of the pore fluid are more important in governing resistivity than the conductivity of the constituent mineral grains. In situations where the porous rocks lie well above the water table and the fraction of the pores filled with fluid is negligibly small, mineralization starts to contribute. Igneous rocks tend to have higher resistivity than sediments. Lavas and tuffs have very high values ranging from 10^2 to 5×10^4 and from 2×10^2 to $10^5 \Omega\text{m}$, respectively, whereas unconsolidated wet clay is known to have resistivity as low as $\sim 20 \Omega\text{m}$. In electrical resistivity survey the current is passed into the ground by means of the current electrodes, electric potential is set up at the surface which is then measured across the potential electrodes, the potential distribution at the surface thus varies as a result of subsurface variation productivity, which alters the flow within the earth, thus the electric potentials at the surface varies. Factors that determine the extent to which the potential at the surface is affected are shape, size, location and conductivity within the ground. The depth penetrated by the current is directly proportional to the current electrode spacing, it also depends on the layering (Telford et al., 1995). If the earth is homogeneous the resistivity measured is called TRUE resistivity, otherwise it is apparent resistivity and this is weighted average of the resistivity of various formations (Osemiekhian et al., 1994). In homogeneous

and isotropic medium, the potential due to a single point current source such as the current electrode A or B, satisfy Laplace equation.

Laplace Equation in spherical polar coordinate for the potential is given by;

$$\frac{d}{dr} \left(\frac{r^2 dv}{dr} \right) + \frac{1}{r^2} \sin\theta \frac{d}{d\theta} \left(\sin\theta \frac{dv}{d\theta} \right) + \frac{1}{r^2} \sin^2\theta \frac{d^2v}{d\varphi^2} = 0$$

Potential varying with r only, so the derivatives with respect to θ and $\varphi = 0$

Hence;

$$\frac{d}{dr} \left(r^2 \frac{dv}{dr} \right) = 0$$

On applying the boundary conditions that $V = 0$ as $r \rightarrow \infty$ and the path of current flow into the ground is hemispherical, the potential function is given by;

$$\frac{d}{dr} \left(\frac{r^2 dv}{dr} \right) = 0 \quad (2.5)$$

Integrating equation (2.4) we have:

$$V = -\frac{A}{r} + B \quad (2.6)$$

Where A and B are constants of integration

Applying boundary condition, $V = 0$ as $r \rightarrow \infty$ then, $B = 0$

Equation (2.3) then becomes

$$V = \frac{A}{r} \quad (2.7)$$

Considering a sphere of radius, r with elemental area, ds and current density, J the current I, flowing is given by;

$$I = J \cdot ds$$

Where I = current density

ds = surface area

But J and ds are normal (angle between them is equal to 0) to the spherical surface and hence

$J \cdot ds$

$$= J \cdot ds \cos 0$$

$$= J \cdot ds$$

The path of current flow into the ground is hemispherical, measurement of V takes place at the same level and the medium is isotropic then,

$$ds = 2\pi r^2$$

$$= \sigma \cdot E \cdot 2\pi r^2 = 2\pi r^2 \sigma \left(-\frac{dv}{dr} \right) \quad (2.8)$$

Hence $V = -\frac{A}{r}$

$$\frac{dv}{dr} = \frac{A}{r^2} \quad (2.9)$$

Combining equation (2.8) and (2.9) becomes;

$$V = 2\pi r^2 \sigma \left(-\frac{A}{r^2} \right) \quad (2.10)$$

$$V = -\frac{I}{2\pi r} \quad (2.11)$$

Substituting equation (2.10) into equation (2.9) gives;

$$V = \rho \frac{I}{2\pi r} \quad (2.12)$$

$$\rho = \frac{2\pi r V}{I} \quad (2.13)$$

The above equation (2.12) is the fundamental equation for electrical prospecting

where

ρ = resistivity in, Ωm

V = Voltage in volts

I = current in, ampere

r = current potential electrode separation in m.

For homogeneous ground, the resistivity values calculated from measurements made at each station is term apparent resistivity, which is weighted average of resistivity of the various layers penetrated by the current (Telford et al., 1995).

2.2.1 Currents and voltages in a uniform Earth

In order to derive a relation between measurements (I, V and geometry) and the required physical property (resistivity or), we must start by identifying how these parameters relate to electric field strength, E (Volts per meter), current density, J (Amps per unit area), and resistivity $\rho(\Omega m)$ in the three dimensional situation of a field survey (the introduction defines resistivity and conductivity). Consider first a uniform Earth and one electrode, which is pumping a current, I, into the ground. We want to find the electric potential within the ground at a distance, r, from the current source. The current density in the ground is related to source current injected, and the potential measured at a surface defined by, r, is related to the electric field that exists in the ground because of the current which flows radially outward from its point source. These two relations will be combined with the 3D form of Ohm's law to end up with an expression for conductivity (the physical property we want) in terms of the current source, measured potential, and the distance. First, by symmetry the current density out of the hemisphere of radius, r, is

$$J = \frac{I}{2\pi r^2} \quad (2.14)$$

and the current is flowing in a radial direction. Since $J = \sigma E$ (Ohm's Law), the electric field must also be pointing radially outward. The relationship between the electric field and the potential is

$$E = -\frac{dV(r)}{dr} \quad (2.15)$$

Combining the expression for E, Ohm's Law and equation 1, we have

$$J = -\sigma \frac{dV(r)}{dr} = \frac{I}{2\pi r^2} \quad (2.16)$$

$$\frac{dV(r)}{dr} = \frac{-I}{2\pi\sigma r^2}$$

If we integrate,

$$V(r) = \frac{I}{2\pi\sigma r} + C \quad (2.17)$$

Choose $v(\infty) \Rightarrow C = 0$

So the potential due to a point current electrode at the surface is:

$$V(r) = \frac{I}{2\pi\sigma r} \quad (2.18)$$

The electric potential inside the earth caused by the radial flow of current is illustrated in the diagram below.

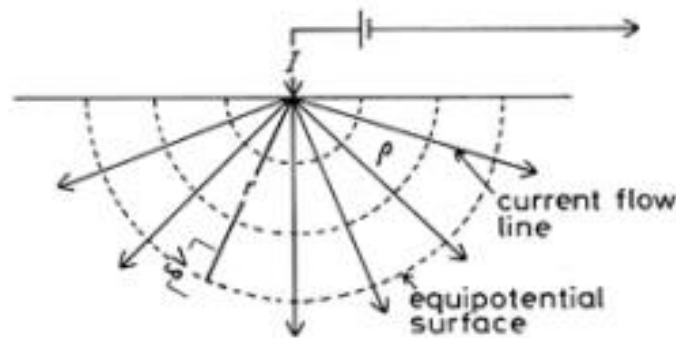


Figure 2.1 Electric potential inside the earth

At the surface, where measurements are made, the potential is infinite at the current electrode because $r=0$, and it decays with distance.

2.2.2 Two electrode current sources

In a geophysical survey, current is injected into the ground using two electrodes. It is convenient to label the electrodes as

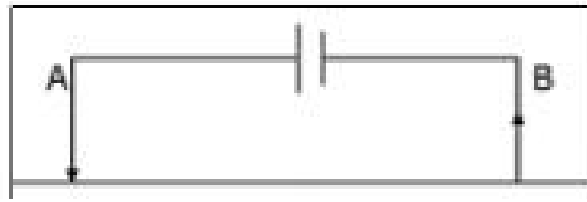


Figure 2.2: current electrode

- A. Positive current electrode (carries a current $+I$)
- B. Negative current electrode (carries a current $-I$)

For a uniform Earth, lines of current flow are shown in red in the figure to the right, and corresponding lines of equal potential (equipotential lines) are shown in black. Instead of the current flowing radially out from the current electrodes, it now flows along curved paths connecting the two current electrodes. Six current paths are shown. Between the surface of the earth and any current path we can compute the total proportion of current encompassed. The table below shows the proportion for the six paths shown (current path 1 is the top-most path and 6 is the bottom-most path).

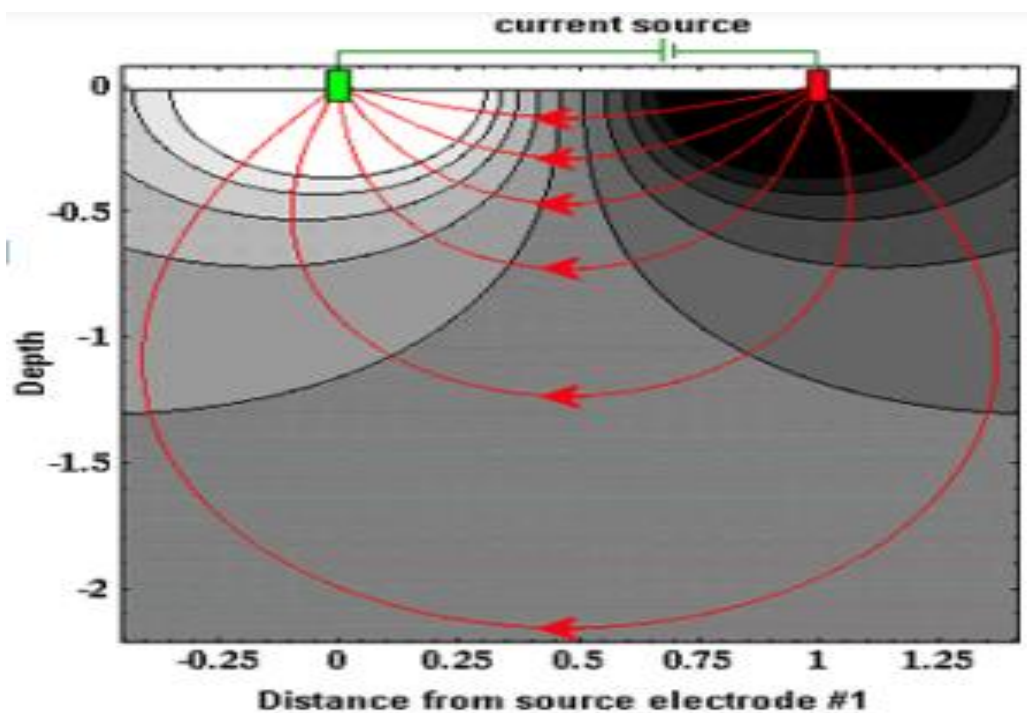


Figure 2.3: graph of the current flow into the ground flows through rock at depths shallower than or equal to the current electrode spacing.

Table 2.2: the proportion for the six paths (current path 1 is the top-most path and 6 is the bottom-most path).

Current Path	% of Total Current
1	17
2	32
3	43
4	49
5	51
6	57

From these calculations and the graph of the current flow shown above, notice that almost 50% of the current placed into the ground flows through rock at depths shallower than or equal to the current electrode spacing. The graph shown below plots the potential that would be measured along the surface of the earth for a fixed 2-electrode source. The voltage we would observe with our voltmeter (between purple electrodes) is the difference in potential at the two voltage electrodes, ΔV .

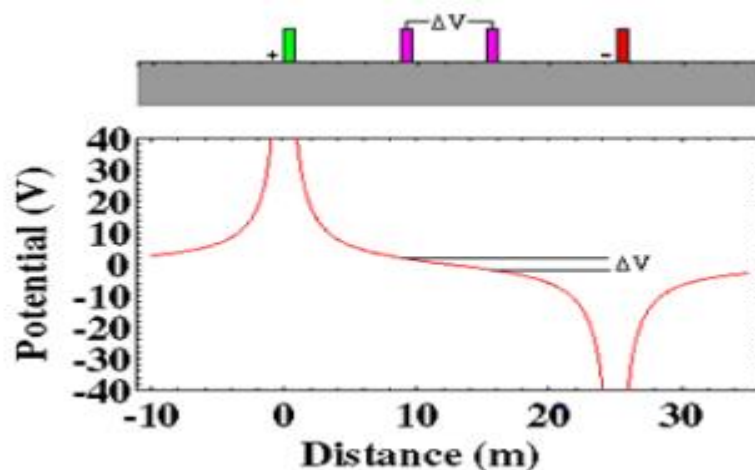


Figure 2.4: voltage Electrode

Practical surveys if there are two current (source) electrodes, the potential is the superposition of the effects from both. In a practical experiment (figure above), one electrode, A, is the positive side of a current source, and the other electrode, B, is the negative side. The current into each electrode is equal, but of opposite sign. For a practical survey, we need two electrodes to measure a potential difference. These are M, the positive terminal of the voltmeter (the one closest to the A current electrode), and N, the negative terminal of the voltmeter.

The measured voltage is a potential difference ($V_M - V_N$) in which each potential is the superposition of the effects from both current sources:

$$\Delta V = V_M - V_N$$

$$V_M = \frac{I\rho}{2\pi} \left\{ \frac{1}{r_{AM}} - \frac{1}{r_{BM}} \right\} \quad \dots \text{so } \dots \quad \Delta V = \frac{I\rho}{2\pi} \left\{ \frac{1}{r_{AM}} - \frac{1}{r_{BM}} - \frac{1}{r_{AN}} + \frac{1}{r_{BN}} \right\}$$

$$V_N = \frac{I\rho}{2\pi} \left\{ \frac{1}{r_{AN}} - \frac{1}{r_{BN}} \right\} \quad \Delta V = I\rho G$$

2.2.3 Apparent resistivity

We are finally in a position to express the thing we want (a physical property) in terms of parameters we either know or measure (current, voltage and geometry). Using two potential electrodes placed between two current electrodes, the flow of current in homogenous isotropic earth, of constant resistivity, is described below. Another term that is frequently found used is the so-called surface resistivity. This is the value of apparent resistivity, obtained with small spacing. Obviously it is equal to the true surface resistivity only when the ground is uniform over a volume of approximately the same dimensions as that of the electrode separation (Loke, 2000). Rearranging the last expression above, we can define apparent resistivity as the halfspace resistivity which produces the observed potential from a particular electrode geometry:

$$\rho_a = \frac{\Delta V}{IG} \tag{2.19}$$

Similarly, the apparent conductivity is

$$\sigma_a = \frac{1}{\rho_a} = \frac{IG}{\Delta V} \quad (2.20)$$

Apparent resistivity is the resistivity derived using only the known current, measured voltage, and array geometry. It is the earth's true resistivity only when the earth (within range of the measurements) is a uniform halfspace. When the earth is more complicated, the measured apparent resistivity will be less than the maximum and more than the minimum true (or intrinsic) resistivities that are within range.

2.2.4 The essence of interpreting resistivity surveys is to find the true distribution of intrinsic resistivities by interpreting the pattern of apparent resistivities that were measured.

Now we can find simple relations between all our known and measured quantities and a useful physical property, namely the apparent resistivity. We only need expressions for the geometric factor based upon electrode geometry. G is easily found if the four distances take on convenient values. For example, if electrodes are spaced equally by a distance a , then, using the figure and relation for V above,

$$G = (1/a - 1/2a - 1/2a + 1/a)/2 = 1/2a.$$

This is the case for the "Wenner" array shown in Figure 6, which summarizes the geometric factor for a variety of common electrode configurations. Note that in this figure, $k=1/G$.

<p style="text-align: center;">Wenner</p> <p style="text-align: center;">$k = 2 \pi a$</p>	<p style="text-align: center;">Wenner Beta</p> <p style="text-align: center;">$k = 6 \pi a$</p>
<p style="text-align: center;">Wenner Gamma</p> <p style="text-align: center;">$k = 1.5 \pi a$</p>	<p style="text-align: center;">Pole - Pole</p> <p style="text-align: center;">$k = 2 \pi a$</p>
<p style="text-align: center;">Dipole - Dipole</p> <p style="text-align: center;">$k = \pi n(n+1)(n+2)a$</p>	<p style="text-align: center;">Pole - Dipole</p> <p style="text-align: center;">$k = 2 \pi n(n+1)a$</p>
<p style="text-align: center;">Schlumberger</p> <p style="text-align: center;">$k = \pi n(n+1)a$</p>	<p style="text-align: center;">Equatorial Dipole - Dipole</p> <p style="text-align: center;">$k = 2 \pi a s / (s - a)$ $s = (a^2 + b^2)^{0.5}$</p>
<p>NOTES: k = geometric factor C = current source electrodes P = potential (measuring) electrode a = electrode separation; n = an integer</p>	

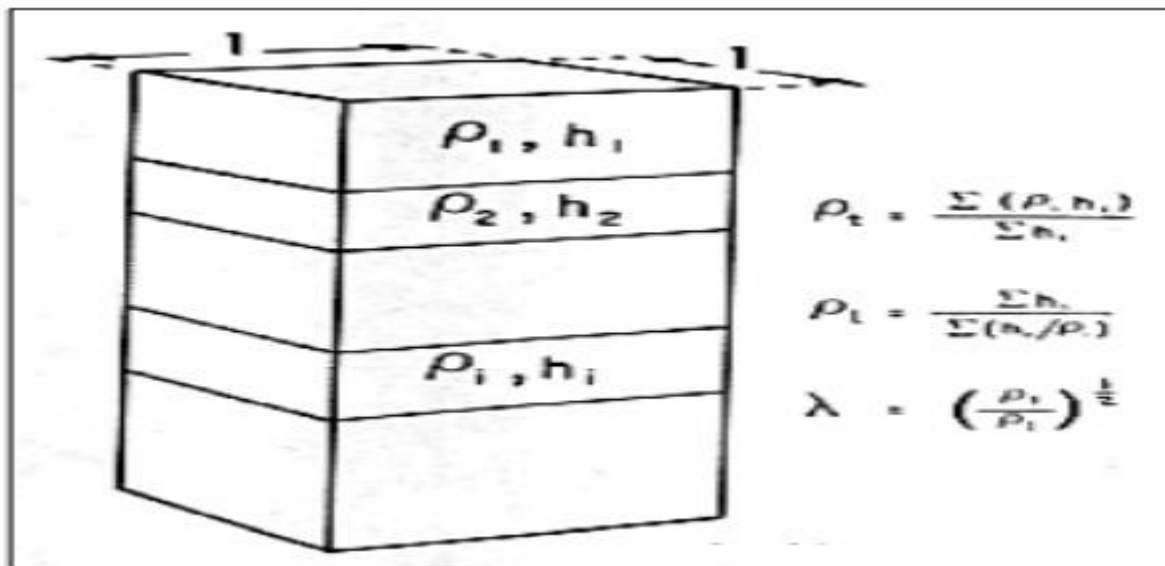
Figure 2.5: Array configuration and their geometric factors

2.2.5 Anisotropic ground

Structural anisotropy (for example, layering or fracturing) causes the simple form of Ohm's law to break down because current flow is not necessarily parallel to the forcing electric field. Instead of simply writing as $\mathbf{J} = \sigma \mathbf{E} = -\sigma \nabla V$, we have to write

$$J_i = -\sigma_{ik} \frac{\partial V}{\partial x_k} \quad i, k = 1, 2, 3.$$

In homogeneous ground with single current and potential electrodes, the expression for V (voltage) in terms of resistivity and distance from the current source is $V = I\rho/2\pi r$ (which was shown above). In anisotropic ground, there are different values of resistivity for the horizontal and a vertical direction. The expression for voltage in terms of the two resistivities and distance is $V = -I\rho_h\lambda/2\pi r$ where $\lambda = (\rho/\rho_h)^{1/2}$ is called the coefficient of anisotropy. See the table below for some values of λ encountered in common geological materials.



Rock type	Coefficient of anisotropy
Volcanic tuff, Eocene and younger, from Nevada	1.10-1.20
Alluvium, thick sections from the southwestern United States	1.02-1.10
Interbedded limestones and limey shales from northeastern Colorado	2.0 -3.0
Interbedded anhydrite and shale, northeastern Colorado	4.0 -7.5
Massive shale beds	1.01-1.05
Interbedded shale and sandstone	1.05-1.15
Baked shale or low-rank slate	1.10-1.60
Slates	1.40-2.25
Bitumenous coal and mudstone	1.7 -2.6
Anthracite coal and associated rocks	2.0 -2.6
Graphitic slate	2.0 -2.8

Figure 2.6: coefficient of anisotropy for layered rocks (after Keller and Frischknecht, 1982)

2.3 ELECTRODE CONFIGURATION IN RESISTIVITY SURVEY

The electrical resistivity method involves the measurement of the apparent resistivity of soils and rock as a function of depth or position. The resistivity of soils is a complicated function of porosity, permeability, ionic content of the pore fluids, and clay mineralization. Electrode configuration (electrode array) is a geometrical pattern of electrodes used in electrical sounding, constant-separation traversing, and induced polarization surveys. Usual configurations comprise two current electrodes and two potential electrodes whose separations are known and defined by a geometric factor. Common arrays configuration includes Schlumberger, Wenner, Pole- Pole, Dipole- Dipole, etc. Each electrode array has its

own geometric factor. The apparent resistivity measured is not affected by the array employed, that is, the apparent resistivity is same irrespective of the array used. The general geometric factor equation which geometric factor arrays are deduced from is described below;

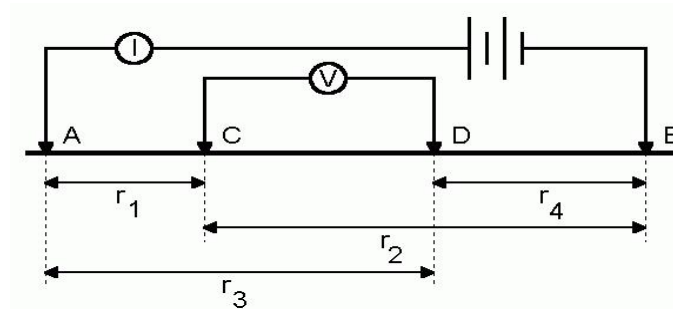


Figure 2.7: Electrode configuration in electrical resistivity surveys

AB = Current electrodes spacing in, meters

CD = Potential electrodes spacing in, meters

Potential at C due to A and B is;

$$C = \rho \frac{1}{2\pi} \left[\frac{1}{r_1} + \frac{1}{r_4} \right] \quad (2.21)$$

Potential at D due to A and B is;

$$D = \rho \frac{1}{2\pi} \left[\frac{1}{r_2} + \frac{1}{r_3} \right] \quad (2.22)$$

The potential difference between C and D is therefore given by;

$$V_C - V_D = V = \rho \frac{1}{2\pi} \left[\frac{1}{r_1} + \frac{1}{r_4} - \left(\frac{1}{r_2} + \frac{1}{r_3} \right) \right] \quad (2.20)$$

Thus,
$$K_a = \frac{1}{2\pi} \left[\frac{1}{r_1} + \frac{1}{r_4} - \left(\frac{1}{r_2} + \frac{1}{r_3} \right) \right] \quad (2.21)$$

This is the geometric factor for any array system. This equation is based on the assumption that the ground is homogeneous and isotropic.

2.3.1 Wenner Array

Wenner electrode array is an electrode configuration in which four electrodes are deployed in a line, with equal spacing between the two potential electrodes, and between each current electrodes and its nearest potential electrode. Its geometric factor (K_g) is $2\pi a$, where a is defined for each case. The Wenner array has five variations, three referred to as the tri-potential method with α , β , and γ configurations, one as the Lee partitioning method (which has a fifth electrode at the array centre acting as a third potential electrode), and one as the Offset Wenner electrode array, which reduces the effects of lateral in-homogeneities.

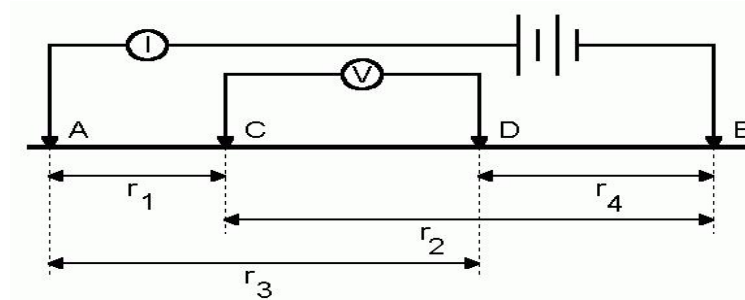


Figure 2.8: Wenner Array

$$K_a = \frac{1}{2\pi} \left[\frac{1}{r_1} + \frac{1}{r_4} - \left(\frac{1}{r_2} + \frac{1}{r_3} \right) \right] \quad (2.22)$$

The specification is given as;

$r_1 = a$, $r_4 = a$, $r_2 = r_3 = 2a$, $AB = 3CD = 3a$ (wenner field condition), with this we get the wenner geometric factor equation as;

$$K = \frac{1}{2\pi a} \quad (2.23)$$

Combining the geometric factor with potential difference, $V = \rho K I$, the apparent resistivity of the formation using wenner array is given by;

$$\rho_a = 2\pi a \frac{V}{I} \quad (2.24)$$

2.3.2 Schlumberger Array

Schlumberger array is an electrode configuration in which the spacing of the two potential electrodes is less than one-fifth of the distance between the Centre of the array and one current electrode. Schlumberger array was proposed by Conrad Schlumberger, it is the most widely used array in electrical prospecting, the electrode spacing are equal (Loke,2003)

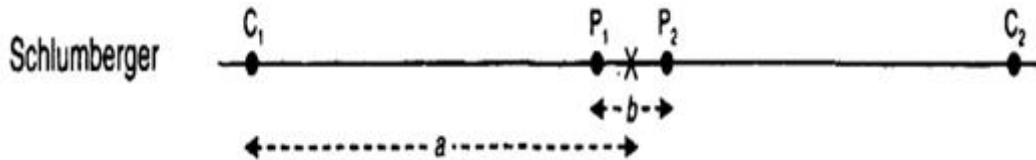


Figure 2.9: Schlumberger Array

$Rr_2 = r_3, r_1 = r_4, AB \geq 5 CD$ (field condition)

Putting the field specifications into array geometrical factor equation,

$$K_a = \frac{1}{2\pi} \left[\frac{1}{r_1} + \frac{1}{r_4} - \left(\frac{1}{r_2} + \frac{1}{r_3} \right) \right] \quad (2.25)$$

The Schlumberger array geometrical factor is given by;

$$K = \frac{1}{2\pi} \left(\frac{1}{r_1} - \frac{1}{r_2} \right) \quad (2.26)$$

For the fact that $r_1 = \frac{AB}{2} - \frac{CD}{2}$, $r_2 = \frac{AB+CD}{2}$,

The geometric factor becomes;

$$K = \pi CD \left[\left(\frac{L}{CD} \right)^2 - 0.25 \right] \quad (2.27)$$

Where $L = \frac{AB}{2}$

The apparent resistivity measured using the system is given by

$$\rho = \frac{KV}{I} \left[\left(\frac{L}{CD} \right)^2 - 0.25 \right] \quad (2.28)$$

CHAPTER THREE

MATERIALS AND METHODOLOGY

3.1 MATERIALS

The data was acquired using the following equipment and accessories;

1. PASI Terrameter 16GL model
2. Thirty-one metal electrodes
3. Four hammers for driving the electrodes in the ground
4. Crocodile clips
5. Two measuring tapes for measuring the distances for the different electrode spacing
6. Global Positioning System 72 (GPS) for finding the position and elevation of the survey point

7. Power supply- 12V 60Ah battery
8. Umbrella
9. Four reels of 2 blue and 2 red coloured electric cable
10. Base map and
11. Data sheet for recording the field data

3.2 EQUIPMENT USED FOR THE FIELD WORK

1. **Metal electrodes:** The electrodes used to inject current into the ground are nearly always metal stakes, which in dry ground may have to be hammered into depths of more than 50 cm and be watered to improve contact. Where contact is very poor, salt water and multiple stakes may be used. In extreme cases, holes may have to be blasted through highly resistive caliche or laterite surface layers. Pointed lengths of angle-iron are only slightly less robust and have larger contact areas. Problems can arise at voltage electrodes, because polarization voltages are generated wherever metals are in contact with the groundwater. However, the reversal of current flow that is routine in conventional DC surveys generally achieves acceptable levels of cancellation of these effects. Voltage magnitudes depend on the metals concerned. They are, for instance, small when electrodes are made of stainless steel.
2. **Measuring Tape:** This is a long roll or strip of plastic that is marked off in inches, centimeter, meter and feet. It is used to measure the length of spread of both the potential and current electrodes. In cases where the length of the spread is exhausted and there are still distances to be covered, measured distances on the ground can be marked, so that the tape is now available to cover the remaining distance.
3. **Cables:** The cables used are traditionally single core, multi-strand copper wires insulated by plastic or rubber coatings. Thickness is usually dictated by the need for mechanical strength rather than low resistance, since contact resistances are nearly always very much higher than cable resistance. Steel reinforcement may be needed for long cables. The cables incorporate heavy gauge conductors with excellent insulation

to ensure good survey results. The cables are expandable for deeper penetration by connecting them in series with a cable joint. The cables are wound on reels.

4. **Pasi Earth Resistivity Meter:** It is light weight and has waterproof, rugged cast aluminum casing. It is a Signal Averaging System. This is a method whereby consecutive readings are taken automatically and the results are averaged continuously.
5. **Battery:** This is used to power the Pasi Earth resistivity meter. It is also the source of the current which is sent into the earth, from which the potential difference across the potential electrodes is measured.
6. **Hammer:** The hammer was used to drive the current electrode into the earth subsurface.
7. **Global Positioning System (GPS):** A GPS signal is used to calculate precise location, altitude, and velocity, as well as the current time of a geographical area. This is needed for accurate analysis of the position of subsurface anomalies.

Some of these instruments are shown in the pictures below.



Figure 3.1: Pasi Earth Resistivity Meters



Figure 3.2: A Global Positioning System



Figure 3.3: Measuring Tape and electrodes.



Figure 3.4: Hammer

3.3 FIELD SURVEY METHOD

The data for this project work was acquired using the PASI Earth Resistivity meter (Terrameter). The Wenner-Schlumberger hybrid array was employed. The results were used to create 2D images of sub-surface geology along a profile with RES2DINV software. Apparent resistivity results gathered by the 2-D dc-resistivity equipment were processed to generate a model-section of subsurface resistivity that represents the true subsurface resistivity variation.

Wenner-Schlumberger configuration is a configuration with a constant system of spacing rules with a note of factor "n" as this configuration is the comparison of the distance between C_1 - P_1 (or C_2 - P_2) electrodes with spaces between P_1 - P_2 . If the distance between electrodes the potentials (P_1 and P_2) are "a" then the distance between the current electrode (C_1 and C_2) is $2na + a$. The resistivity determination process uses 4 electrodes placed in a straight line. This configuration is a combination of the Wenner configuration and Schlumberger configuration. In the measurement by the spacing factor $(n) = 1$, the Wenner-Schlumberger configuration is similar to the measurement in the Wenner configuration (distance between electrode = a), but on the measurement with $n = 2$ and so on, the Wenner-Schlumberger configuration is the same as the Schlumberger configuration. The current electrode and the potential electrode are greater than the distance between the potential electrodes).

3.4 MEASUREMENT PROCEDURE

1. Fill out site details on standard data sheet.
2. Check the battery to ensure it is still charged,
 - 11.5 volts (use battery check on the SAS300)
3. Set PC switch towards the BGS label.
 - Start with a current setting of 20mA. Always use maximum current obtainable and decrease as required.
4. Set the resistivity range either to 1 ohm or 100 ohms
5. Take measurements for A, C, D1, D 2 and B at settings 1 to 9.
 - If an error code is displayed refer to the error code sheet. (e.g. error message "1" indicates that a current electrode is disconnected)
6. Record the measured resistance
 - make sure consistent readings are obtained
 - Note the units recorder e.g. mohms, ohms or kohms
 - Use the standard data sheet
 - Measure the direction of the cable line using a compass and record on the data sheet.

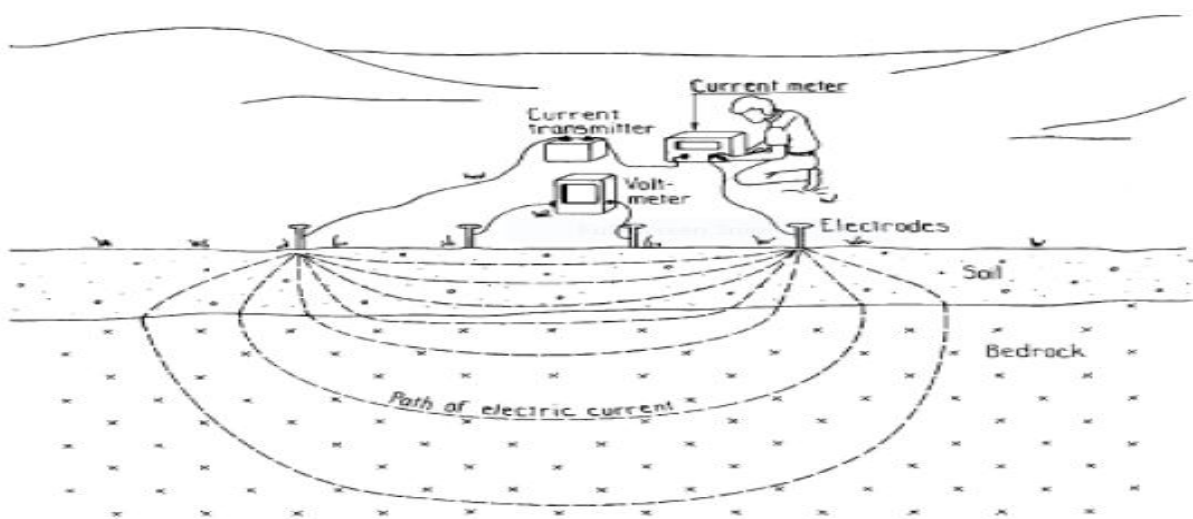


Figure 3.5: Principle of resistivity measurement (modified from Robinson and Coruh, 1988).

3.4.1 Field calculations

Field calculation of the Wenner-Schlumberger geometric factor, Resistivity should be carried out using the field sheet. Calculations involve finding the average of measurements RD1 and RD2 multiplying by $\pi n(n+1)a$ (a = spacing). Plot values on log-log graph paper and draw a curve to fit the plotted points.

CHAPTER FOUR

RESULT AND DISCUSSION

4.1 RESULT

Table 4.1: 2-D Wenner-Schlumberger Electrical Resistivity Field Record – Traverse one

ARRAY TYPE	Wenner-Schlumberger Array	DATE	
INSTRUMENT USED	Pasi Earth Resistivity Meter	STATE	Edo
LOCATION	UBTH	LGA	Ovia North East
OBSERVER			

Traverse 1 Long 005°36'01.62" Lat 06°27'40.98" Elev 98m

Traverse 1 a = 10m (CD)					
C1	P1	P2	C2	$\rho(\Omega)$	$\rho(\Omega m)$
0	5	10	15	1.8	56.556
5	10	15	20	1.6	50.272
10	15	20	25	1.3	40.846
15	20	25	30	1.1	34.562
20	25	30	35	1.8	56.556
25	30	35	40	1.8	56.556
30	35	40	45	1.5	47.13
35	40	45	50	1.5	47.13
40	45	50	55	1.5	47.13
45	50	55	60	1.2	37.704
50	55	60	65	1.3	40.846
55	60	65	70	1.2	37.704
60	65	70	75	1.2	37.704
65	70	75	80	1.2	37.704
70	75	80	85	1.1	34.562
75	80	85	90	1.2	37.704
80	85	90	95	1.3	40.846
85	90	95	100	1.5	47.13
Traverse 1 a = 10m					
C1	P1	P2	C2	$\rho(\Omega)$	$\rho(\Omega m)$
0	10	20	30	1.2	75.408
5	15	25	35	0.441	27.71244
10	20	30	40	0.464	29.15776
15	25	35	45	0.621	39.02364
20	30	40	50	0.268	16.84112
25	35	45	55	0.244	15.33296
30	40	50	60	0.265	16.6526
35	45	55	65	0.512	32.17408
40	50	60	70	0.621	39.02364
45	55	65	75	0.868	54.54512
50	60	70	80	0.749	47.06716
55	65	75	85	0.644	40.46896
60	70	80	90	0.621	39.02364
65	75	85	95	0.487	30.60308
70	80	90	100	0.468	29.40912
Traverse 1 a = 10m					
C1	P1	P2	C2	$\rho(\Omega)$	$\rho(\Omega m)$
0	15	30	45	0.611	57.593
5	20	35	50	0.621	58.535
10	25	40	55	0.615	57.970
15	30	45	60	0.768	72.392
20	35	50	65	0.511	48.167
25	40	55	70	0.682	64.285
30	45	60	75	0.748	70.506
35	50	65	80	0.568	53.540
40	55	70	85	0.564	53.163
45	60	75	90	0.598	56.367

50	65	80	95	0.679	64.003
55	70	85	100	0.668	62.966
Traverse 1 a = 10m					
C1	P1	P2	C2	$\rho(\Omega)$	$\rho(\Omega m)$
0	20	40	60	0.468	58.818
5	25	45	65	0.556	69.878
10	30	50	70	0.486	61.080
15	35	55	75	0.698	87.725
20	40	60	80	0.621	78.047
25	45	65	85	0.544	68.370
30	50	70	90	0.568	71.386
35	55	75	95	0.594	74.654
40	60	80	100	0.486	61.080
Traverse 1 a = 10m					
C1	P1	P2	C2	$\rho(\Omega)$	$\rho(\Omega m)$
0	25	50	75	0.412	64.725
5	30	55	80	0.541	84.991
10	35	60	85	0.411	64.568
15	40	65	90	0.468	73.523
20	45	70	95	0.511	80.278
25	50	75	100	0.312	49.015
Traverse 1 a = 10m					
C1	P1	P2	C2	$\rho(\Omega)$	$\rho(\Omega m)$
0	30	60	90	0.368	69.375
5	35	65	95	0.421	79.367
10	40	70	100	0.268	50.523
Long 005°36'02.19" Lat 06°27'43.92" Elev 100m					

Table 4.2: 2-D Wenner-Schlumberger Electrical Resistivity Field Record – Traverse Two

Traverse 2 Long 005°35'59.58" Lat 06°27'44.75" Elev 103m					
Traverse 3 a = 10m (AD)					
C1	P1	P2	C2	$\rho(\Omega)$	$\rho(\Omega m)$
0	5	10	15	1.6	50.272
5	10	15	20	1.4	43.988
10	15	20	25	1.2	37.704
15	20	25	30	1.3	40.846
20	25	30	35	1.9	59.698
25	30	35	40	1.4	43.988
30	35	40	45	1.2	37.704
35	40	45	50	1.1	34.562
40	45	50	55	1.6	50.272
45	50	55	60	1.4	43.988
50	55	60	65	1.2	37.704
55	60	65	70	1.1	34.562
60	65	70	75	1.1	34.562
65	70	75	80	0.821	25.79582
70	75	80	85	0.816	25.63872

75	80	85	90	1.2	37.704
80	85	90	95	1.3	40.846
85	90	95	100	1.5	47.13
Traverse 3 a = 10m					
C1	P1	P2	C2	$\rho(\Omega)$	$\rho(\Omega m)$
0	10	20	30	1.2	75.408
5	15	25	35	0.661	41.53724
10	20	30	40	0.411	25.82724
15	25	35	45	0.841	52.84844
20	30	40	50	0.812	51.02608
25	35	45	55	0.612	38.45808
30	40	50	60	0.741	46.56444
35	45	55	65	0.716	44.99344
40	50	60	70	0.744	46.75296
45	55	65	75	0.722	45.37048
50	60	70	80	0.621	39.02364
55	65	75	85	0.562	35.31608
60	70	80	90	0.578	36.32152
65	75	85	95	0.451	28.34084
70	80	90	100	0.624	39.21216
Traverse 3 a = 10m					
C1	P1	P2	C2	$\rho(\Omega)$	$\rho(\Omega m)$
0	15	30	45	0.611	57.593
5	20	35	50	0.502	47.319
10	25	40	55	0.441	41.569
15	30	45	60	0.484	45.622
20	35	50	65	0.611	57.593
25	40	55	70	0.584	55.048
30	45	60	75	0.598	56.367
35	50	65	80	0.611	57.593
40	55	70	85	0.486	45.810
45	60	75	90	0.462	43.548
50	65	80	95	0.562	52.974
55	70	85	100	0.466	43.925
Traverse 3 a = 10m					
C1	P1	P2	C2	$\rho(\Omega)$	$\rho(\Omega m)$
0	20	40	60	0.386	48.512
5	25	45	65	0.323	40.595
10	30	50	70	0.344	43.234
15	35	55	75	0.598	75.157
20	40	60	80	0.411	51.654
25	45	65	85	0.311	39.086
30	50	70	90	0.262	32.928
35	55	75	95	0.262	32.928
40	60	80	100	0.241	30.289
Traverse 3 a = 10m					
C1	P1	P2	C2	$\rho(\Omega)$	$\rho(\Omega m)$
0	25	50	75	0.912	143.275
5	30	55	80	0.912	143.275

10	35	60	85	0.946	148.617
15	40	65	90	0.741	116.411
20	45	70	95	0.726	114.055
25	50	75	100	0.566	88.919
Traverse 3 a = 10m					
C1	P1	P2	C2	$\rho(\Omega)$	$\rho(\Omega m)$
0	30	60	90	0.864	162.881
5	35	65	95	0.948	178.717
10	40	70	100	0.786	148.177
Long 005°36'02.19" Lat 06°27'43.92" Elev 100m					

4.2 INTERPRETATION OF RESULTS

The resistivity of common rocks, soils and other materials, resistivity survey gives a picture of the subsurface resistivity distribution. To convert resistivity picture into a geological picture, some knowledge of typical resistivity values for different types of subsurface materials and the geology of the area surveyed, is important.

Table 4.4: Resistivity values of common rocks, soil materials and chemicals (Loke, 2000).

Material	Resistivity (Ωm)
Sandstone	$8 - 4 \times 10^3$
Shale	$20 - 2 \times 10^3$
Limestone	$50 - 4 \times 10^2$
Clay	1 - 100
Alluvium	10 - 800
Ground water (fresh)	10 - 100
Sea water	0.2
Ash	4
Colliery spoil	10 - 20
Pulverized fuel ash	50 - 100
Laterite	800 - 1500
Lateritic soil	120 - 750
Dry sandy soil	80 - 1050
Sand clay/ clayey sand	30 - 215
Sand and gravel	30 - 225

Unsaturated landfill	30 – 100
Saturated landfill	15 – 30
Acid mine water	20
Rainfall runoff	20 – 100
Landfill runoff	< 10 – 50

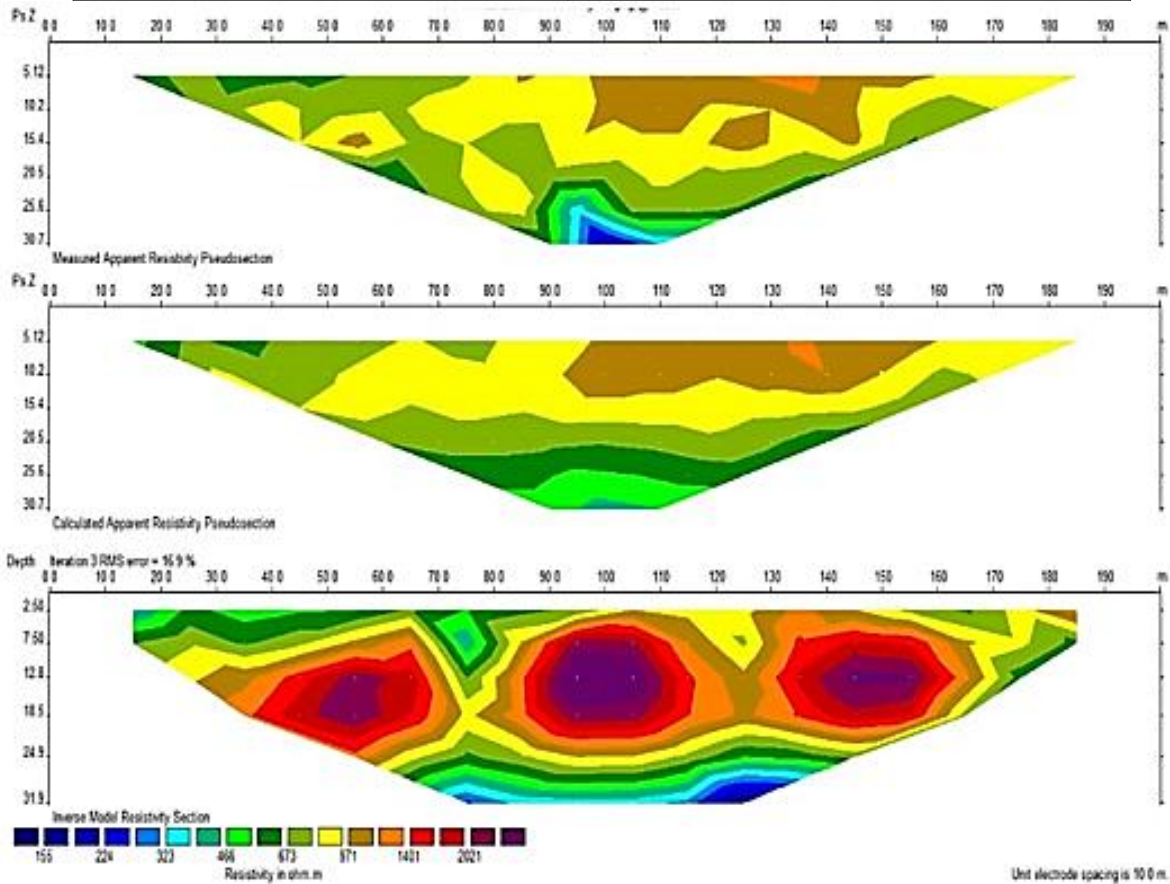


Figure 4.1: Traverse 1 showing the inverse resistivity section

From the 2D image obtained from line 1, it can be seen that laterites and lateritic soils are the major constituents of the survey areas subsurface. The resistivity of laterites ranges from 800-1500 Ω , while that of lateritic soils range from 120-750 Ω m. Thus from the resistivity block section it can be seen that the resistivity of the sub-surface soils corresponds with the resistivity of laterites, thereby confirming the existence of laterites deposits in the survey area, although they are scanty and sparsely distributed. The deposits of laterites and lateritic soils can be seen from depth 2-10m. These accumulation of laterites are not of economic quantity and cannot be mined for economic purposes.

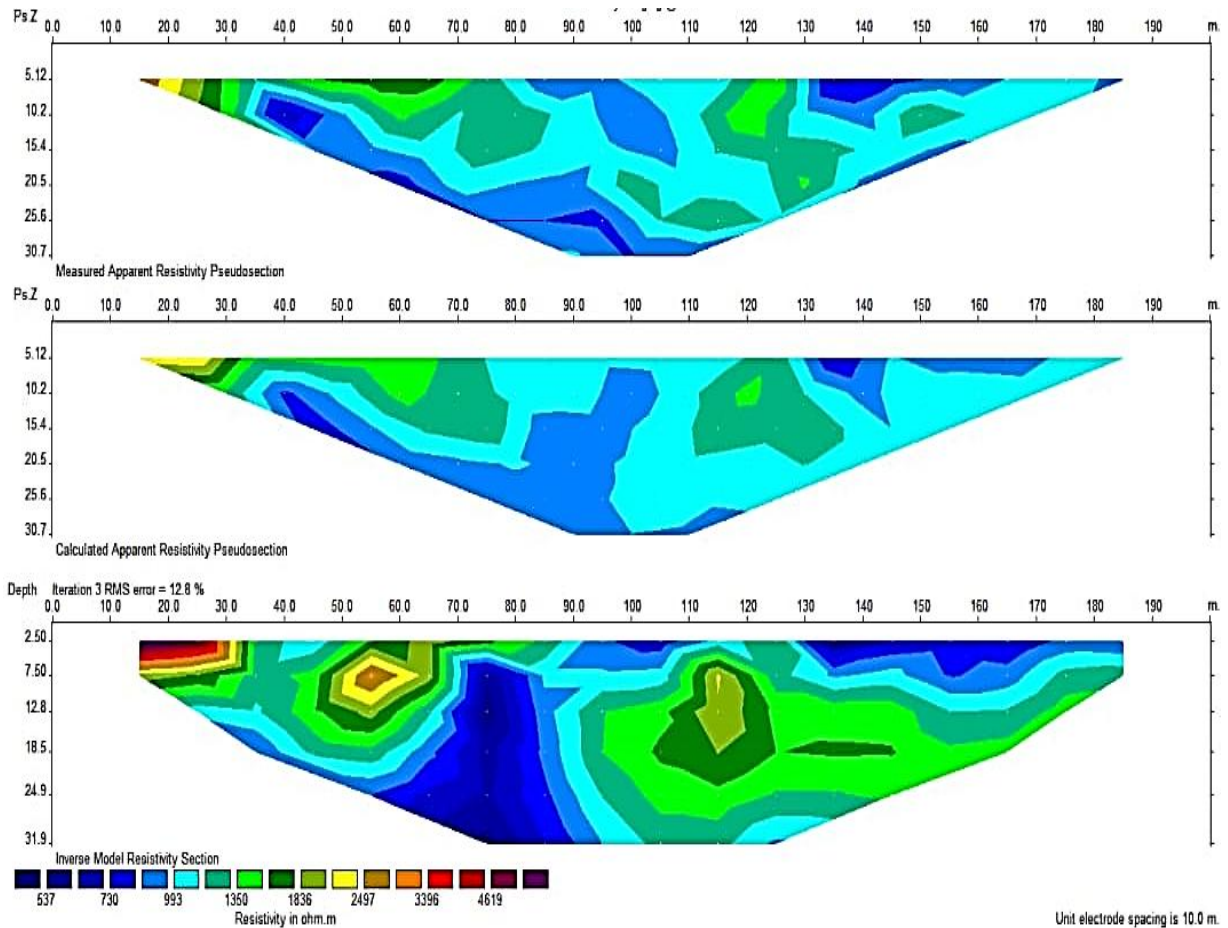


Figure 4.2. Traverse 2 showing the inverse resistivity section

Profile two (2) showed high resistivity region at the top layer which is within the lateral distance of 10 m to 30 m with the resistivity value range of 3396 Ω m to 4619 Ω m. The Inverse model of the profile two (2) is more of low resistivity region which falls within the resistivity value of 537 Ω m to 1000 Ω m. The resistivity of laterites ranges from 800-1500 Ω . The high resistivity region symbolizes a suspected sandstone and limestone because the geophysics signature of high resistivity can be attested in mineralization.

CHAPTER FIVE

FINDINGS, CONCLUSION AND SUGGESTION FOR FURTHER STUDIES

5.1 FINDINGS

1. For traverse 1, the resistivity of laterites ranges from 800-1500 Ω , while that of lateritic soils range from 120-750 Ω m. Thus from the resistivity block section it can be seen that the resistivity of the sub-surface soil corresponds with the resistivity of laterites, thereby confirming the existence of laterites deposits in the survey area.

2. The Inverse model of the profile two (2) show low resistivity region which falls within the resistivity value of 537 Ω m to 1000 Ω m. The resistivity of laterites ranges from 800-1500 Ω .

5.2 CONCLUSION

The 2-D electrical resistivity imaging method has been successfully used to investigate the subsurface structures at the proposed survey areas. This was with a view to investigate the presence of Laterite deposits in the areas. The 2-D electrical resistivity data were acquired from the area using the PASI Earth Resistivity Meter system. The acquired apparent resistivity data was interpreted using the RES2DINV software. The results showed that there are laterite deposits in the survey area for both profile one and two respectively.

5.3 SUGGESTION FOR FURTHER STUDIES

1. Further research should be carried out with an increase in the probing depth so as to determine the lateral and vertical extent of laterites in the survey areas.
2. More than one array system in more than one profile is always necessary before proper inference can be made in reference to structural lithology.

REFERENCES

- Adekunle, A. A. and Adebambo, O. A. 2007.** Petroleum Hydrocarbon Utilization by Fungi Isolated From Detarium senegalense Seeds. Journal of American Science 3(1): 69- 76.
- Adekunle, A.A. and Adeniyi, A.O. 2015.** Hydrocarbon utilization of fungi isolated from Treculia africana (Decene) seeds. African journal of environmental science and technology 9(2):126-135.

- Adekunle, A.A. and Oluyode, T. F. 2005.** Biodegradation of Crude Petroleum and Petroleum Products by fungi isolated from two oil seeds (Melon and soybean seeds). *Journal of Environmental Biology* 26(1): 37-42.
- Ayolabi, E. A, Folorunso, A. F, and Eleyinimi, A. F. 2009.** Applications of 1D and 2D electrical resistivity methods to map aquifers in a complex geologic terrain of foursquare camp, Ajebo, Southwestern Nigeria. *The Pacific J. Science Technology*, 10(2),657–666.
- Barker, R.D. 1978.** The offset system of electrical resistivity sounding and its use with a multicore cable. *Geophysical Prospecting*, **29**, 128-143
- Dahlin, T. 1996.** 2D resistivity surveying for environmental and engineering applications. *First Break*, **14**, 275-284.
- Doust, H. and Omatsola, E. 1990.** Niger-Delta. In: Edwards, J.D. and Santogrossi, P.A., Eds., *Divergent/Passive Margin Basins*, AAPG Memoir 48, American Association of Petroleum Geologists, Tulsa, 239-248.
- Edwards L.S., 1977.** A modified pseudosection for resistivity and induced-polarization. *Geophysics*, 42, 1020-1036.
- Griffiths D.H. and Barker R.D. 1993.** Two-dimensional resistivity imaging and modelling in areas of complex geology. *Journal of Applied Geophysics*, **29**, 211-226.
- Griffiths D.H. and Barker, R.D. 1993.** Two-Dimensional Resistivity Imaging and Modeling in Areas of Complex Geology. *Journal of Applied Geophysics*, 29, 21-26.
- Griffiths D.H., Turnbull J. and Olayinka A.I. 1990.** Two-dimensional resistivity mapping with a computer- controlled array. *First Break* **8**, 121-129.
- Keller G.V. and Frischknecht F.C. 1966.** *Electrical methods in geophysical prospecting.* Pergamon Press Inc., Oxford.
- Kogbe, C. A. 1989.** *Geology of Nigeria.* 2nd Edition, Rock View Ltd., Jos, Nigeria.

- Loke, M.H and Barker R. D. 1996.** Practical Techniques for 3D Resistivity Surveys and Data Inversion. *Geophysical Prospecting*, 44: 499-524.
- Ogunsanwo, O. 1989.** "Some geotechnical properties of two laterite soils compacted at different energies." *Engineering Geology* 26: 261-269.
- Osemeikhian, J. E. A and Asokhia, M. B. 1995.** "Applied Geophysics", Samtos Services, Illupeju, Lagos
- Pidlisecky A, Knight R and Haber E 2006.** Cone-based electrical resistivity tomography; *Geophysics* 71(4) 157–167.
- Sivaramakrishnan J, Asokan A, Sooryanarayana K R, Hegde S S and Benjamin J 2015**
Occurrence of ground water in hard rock under distinct geological setup; *Aquat. Procedia*. 4 706–712.
- Stauble, (1967) and Etu-Efeotor (1981).** The chronostratigraphic units of the Niger delta after Short and.
- Tardy Y 1992.** Diversity and terminology of lateritic probles; In: *Developments in earth surface processes*; Elsevier 2 379–405.
- Telford, W.M., Geldart, L.P. and Sheriff, R.E. 1990.** *Applied Geophysics*, Cambridge University Press, U.K.
- Van Schoor M 2002.** Detection of sinkholes using 2D electrical resistivity imaging. *J Appl Geophys* 50:393–399